Biophysical Chemistry, 48 (1993) 113–122
Elsevier Science Publishers B.V., Amsterdam

BIOCHE 01791

Temperature dependence of Raman vibrational bandwidths in poly(rA) and rAMP

P.A. Terpstra, C. Otto * and J. Greve

University of Twente, Department of Applied Physics, Applied Optics Group, P.O. Box 217, 7500 AE Enschede (The Netherlands)

(Received 19 April 1993; accepted in revised form 24 June 1993)

Abstract

Isotropic and anisotropic spontaneous Raman spectra were obtained from solutions of poly(rA) and rAMP in buffer. The temperature dependence of these spectra was measured to elucidate the influence of macromolecular dynamics and solvent dynamics on the bandwidths of base vibrations in the single stranded polynucleotide poly(rA). The temperature dependence of a bandwidth depends upon the particular vibration under study. The bands can for the larger part be described by Lorentz functions. When fitted by Voigt functions, maximally 10% of each bandprofile of the adenine base vibrations can be attributed to a Gaussian component. The second moment has been determined from the spectra for the 725 cm^{-1} band. From the second moment and the bandwidth, we were able to deduce that the vibrational oscillator is in the fast modulation limit. The determined timescale (perturbation correlation time ≤ 0.13 ps) eliminate perturbations connected to long range diffusion like concentration fluctuations (timescale in the order of 10 ps). The spectra were analyzed by an extensive curve fitting procedure providing accurate bandparameters (position, width and integrated intensity). The 725 cm^{-1} band of adenine has a bandwidth which is dependent upon the degree of polymerization. In rAMP it is 17.6 cm^{-1}, in stacked (i.e. low temperature 5°C) poly(rA) it is 11.5 cm^{-1}. The bandwidth of the adenine vibration at 1336 cm^{-1} cm^{-1} has a temperature dependence which is similar to the intensity changes of the Raman and the absorption hypochromic effect as a function of temperature. The melting transition can therefore be followed by the changes in bandwidth of suitable vibrations.

Keywords: Molecular Dynamics; Solvent dynamics; Raman; Bandwidth; Poly(rA)

1. Introduction

The developments in generation of femtosecond light pulses open many ways to follow fast dynamics in molecular ensembles. Time domain spectroscopy is extremely powerful as it is known [1,2] that by suitable choices of pulse sequences various contributions to the bandwidth, i.e. inhomogeneous versus homogeneous and pure dephasing versus energy relaxation, can be separated. Polarization coherent anti-Stokes Raman spectroscopy (CARS) using subpicosecond pulses [3] was used to separate the contributions of various Raman scattering tensor elements to the final intensity of the coherently generated signal. Reorientational broadening mechanisms showing up in the anisotropic scattering can in this way be

* Corresponding author. Tel.: (+31-53) 893157, fax: (+31-53) 309549.

studied when the decay is compared with that of the isotropic scattering component. The occurrence of a fast pulse substructure in the broadband nanosecond pulse of a Nd–YAG laser may be used to obtain fast dynamics of molecular systems when a twin pair of these incoherent pulses is applied [4]. The time delay between the pairs of pulses is used to monitor the dynamics of excitation vibration(s). Time-resolved spontaneous Raman scattering has been succesfully applied to dilute solutions of molecules. In case of resonant excitation this method can be used to study the excited state dynamics of molecules as for instance β-carotene [5].

By nature, frequency domain spontaneous Raman scattering is also capable to probe fast dynamics in molecular systems. It is sensitive and can therefore also be used in non-resonant excitation of dilute solutions of macromolecular systems that are of direct significance in biophysics. As such, it has not been applied very often probably because of the high complexity of Raman spectra of biological macromolecules. The development of fast and accurate curve-fitting programs, however, enables the quantification of spectral information by suitable bandshape function.

This paper presents a study into the vibrational bandwidths of adenine in the polynucleotide poly(rA). The bandwidths obtained for poly(rA) are compared with those of the mononucleotide rAMP, in the temperature range where poly(rA) gradually changes from a base stacked structure to an unstacked structure. At the ionic concentration used in this study the midpoint of this transition is approximately at 45°C. The changes in the bandwidths are compared with changes in the scattering intensity of vibrational bands. This Raman hyperchromism (i.e. an increase of the scattering cross section upon unstacking of the base molecules) reveals the unstacking of base molecules [6,7]. It will appear that bands of poly(rA) show great differences with rAMP, which shows the effect of secondary structure. Extensive use of curve-fitting procedures to extract reliable information from complicated Raman spectra of polynucleotides appears to be essential.

2. Materials and methods

Poly(rA) (Pharmacia; Lot no.: AA4110p01) and rAMP (Sigma; Lot no.: 90H7215) were used without further purification. The sedimentation constant for poly(rA), $s_{20,w} = 8.8$, yields a chain-length of approximately 600 bases. All measurements reported were obtained in a buffer solution containing 10 mM NaH_2PO_4, 93 mM NaCl and 7 mM Na-cacodylate. The pH of the solution is 7.2 and the nucleotide concentrations were 78 mM. The temperature of the sample was controlled by a heat bath and is accurate to within 0.5°C.

The spectrometer was a Jobin-Yvon Ramanor HG 2S in a 90° setup. The scattered light passes through an analyzer (Spindler & Hoyer 10K: with a suppression ratio of 10^{-4}) which selects vertically polarized light. Photon counting is performed with a Hamamatsu R943-02 Photomultiplier.

The VV- and HV-spectra were obtained quasi simultaneously. After each step of the monochromator (typically 1 cm^{-1}), the scattering intensity was measured of the vertically polarized component, first with an than without a $1/2\lambda$-plate in the excitation path. Measuring time was 15 seconds per spectral point. In this way it was achieved that isotropic and anisotropic Raman spectra are exactly frequency calibrated. The VV- and HV-spectra of poly(rA) were obtained form the measured spectra after subtraction of the respective VV- and HV-spectra of the buffer at the appropriate temperature.

The slitwidth was adjusted in such a way that no further change is observed in the bandwidths while increasing the instrument resolution [8], which resulted in a maximum resolution of 3 cm^{-1}. The full width half maximum (FWHM) of the bands in poly(rA) are typically of the order of 12–20 cm^{-1}. To assure the frequency definition of the spectra, the spectra were obtained in one single scan to avoid spectral impurity due to backlash of the monochromator.

The angle of the $1/2\lambda$-plate was adjusted such that the minimum depolarization ratio was obtained for the chloroform 667 cm^{-1} band. A depolarization ratio of 0.012 was obtained for this band, which compares well with the literature

value of 0.014 [9]. The whole set-up, i.e. collection optics, polarization filter, monochromator and detector, has been intensity calibrated by using a tungsten lamp, the emission of which was modeled as a black-body radiator.

The argon ion laser source is a Spectra-Physics 2025-03. All spectra were obtained with 514.5 nm (19436.3 cm^{-1}) excitation wavelength. The bandwidth of this laser emission line is 6 GHz (0.2 cm^{-1}).

The isotropic and anisotropic Raman spectra were curve-resolved with Lorentz bandshape functions using the fit-program developed by the Mul et al. [10]. This program allows a choice of various bandshape functions, such as Lorentz-, Gauss- or Voigt-functions, but all bands of the adenine base proved to be at least 90% Lorentz. Application of a versatile and fast curve-fitting program is a prerequisite for obtaining quantitative spectroscopic information from complex spectra as will be shown in this paper.

3. Results

From the measured VV and HV spectra, the isotropic and anisotropic spectra can be calculated.

$$I_{iso} = I_{VV} - \tfrac{4}{3} I_{HV}, \quad (1)$$

$$I_{aniso} = I_{HV}, \quad (2)$$

where I_{iso} measures the trace of the polarizability and I_{aniso} the anisotropy. In Fig. 1 the isotropic and anisotropic Raman spectra of rAMP at a temperature of 22°C are shown. From the vibrations at 1336 and 1578 cm^{-1} it can be observed that the correlation time for reorientational motion of the rAMP molecule in solution is 5 picosecond ± 1 ps (see below). No reorientational motion can be observed from the isotropic and anisotropic Raman spectra of poly(rA) (data not shown) suggesting that the reorientation of the

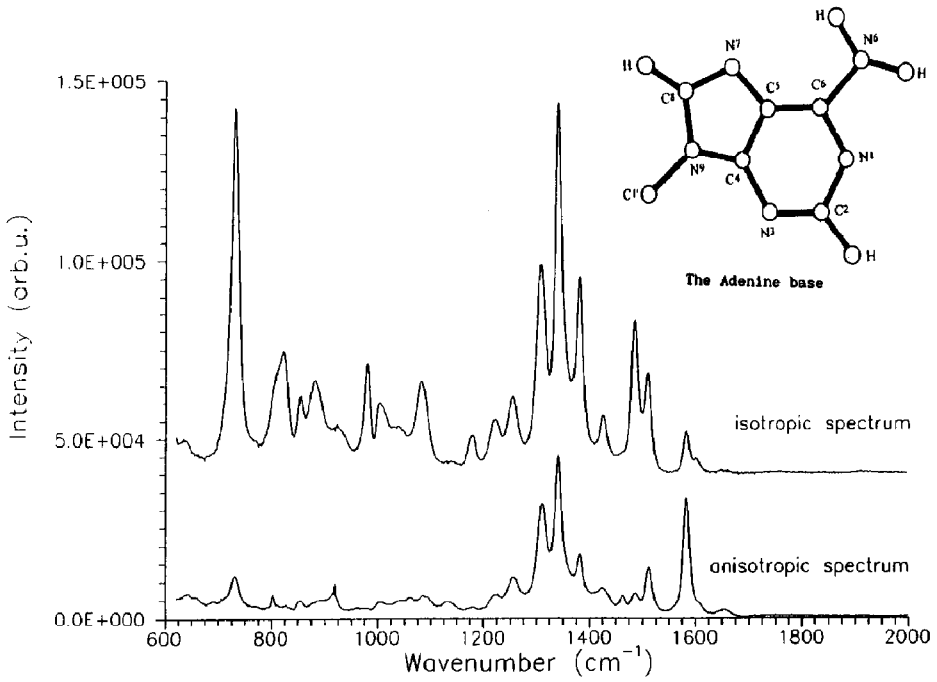

Fig. 1. The isotropic and anisotropic Raman spectra of rAMP at 22°C. The bandwidths of the vibrations at 725, 1336, 1480 and 1505 cm^{-1} in the isotropic spectrum and of the vibration at 1578 cm^{-1} in the anisotropic spectrum have been used to probe the dynamics of the poly(rA) and rAMP (see text). The inset presents the adenine molecule and the numbering of the atoms.

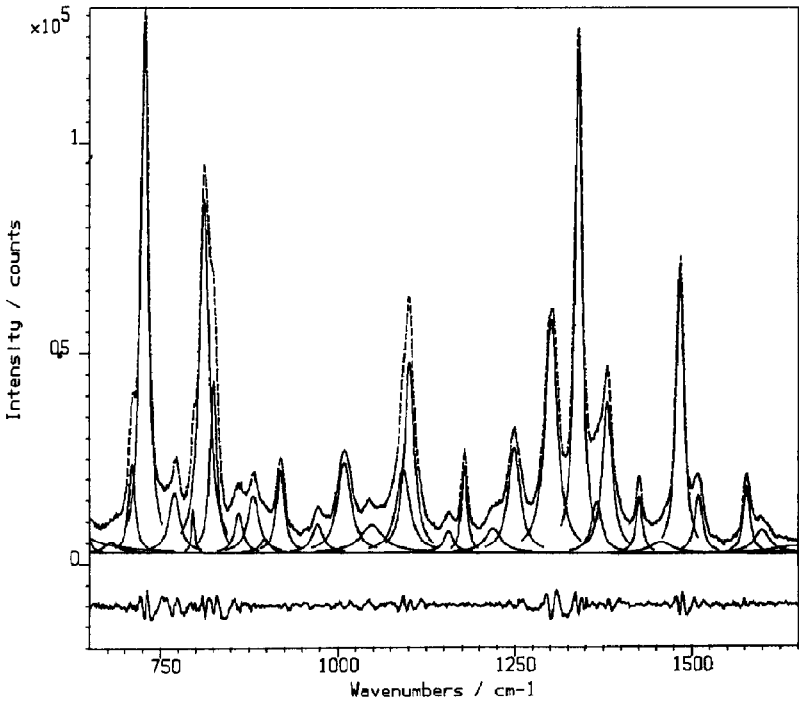

Fig. 2. An example of a curve resolved spectrum of poly(rA) (5°C). The lower curve represents the residue spectrum (original – calculated spectrum) and is a measure for the accuracy of the fit.

base in this polymer is slower than 10 ps. The reorientational motion of the poly(rA) molecule will depend on the number of monomers in the poly(rA), but apparently is orders of magnitude slower than the experimentally resolvable timescale for reorientational motions (0.1 to 10 ps).

At 5°C, the poly(rA) is in a stacked conformation, we observed no further changes in the bandwidths down to −6°C. The unstacking interactions can be followed in the absorption spectrum and in the Raman spectrum by gradually increasing the temperature. In Fig. 2 the curve resolved Raman spectra of poly(rA) at 5°C are presented together with the measured data and the residual spectrum. The low magnitude of the residual spectrum is nearly constant as a function of temperature. The uncertainty in the curve fit is directly leading to an uncertainty in the obtained spectroscopical parameters. In Fig. 3 the absorption hypochromism as a function of temperature is presented together the bandwidth of the vibration at 1336 cm^{-1}. As was already noticed by

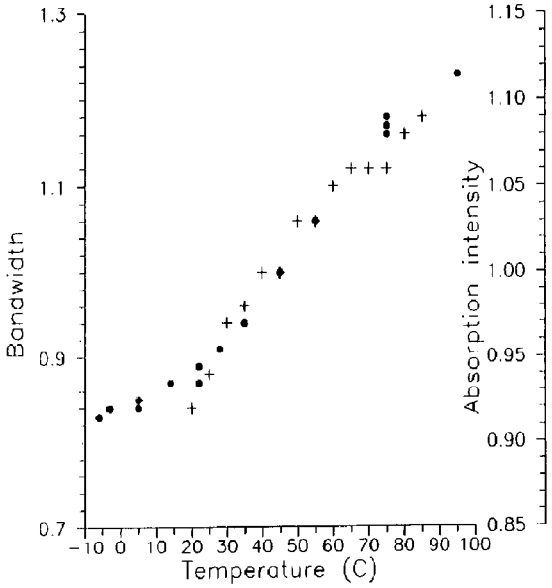

Fig. 3. Hypochromism for poly(rA) as a function of the temperature measured by Absorption intensity at 258 nm (+) and Raman bandwidth for the vibration at 1336 cm^{-1} (·). The figure presents fractional changes. The values at 45°C have been taken as 1. The Raman bandwidth of this vibration follows the melting transition of the polynucleotide.

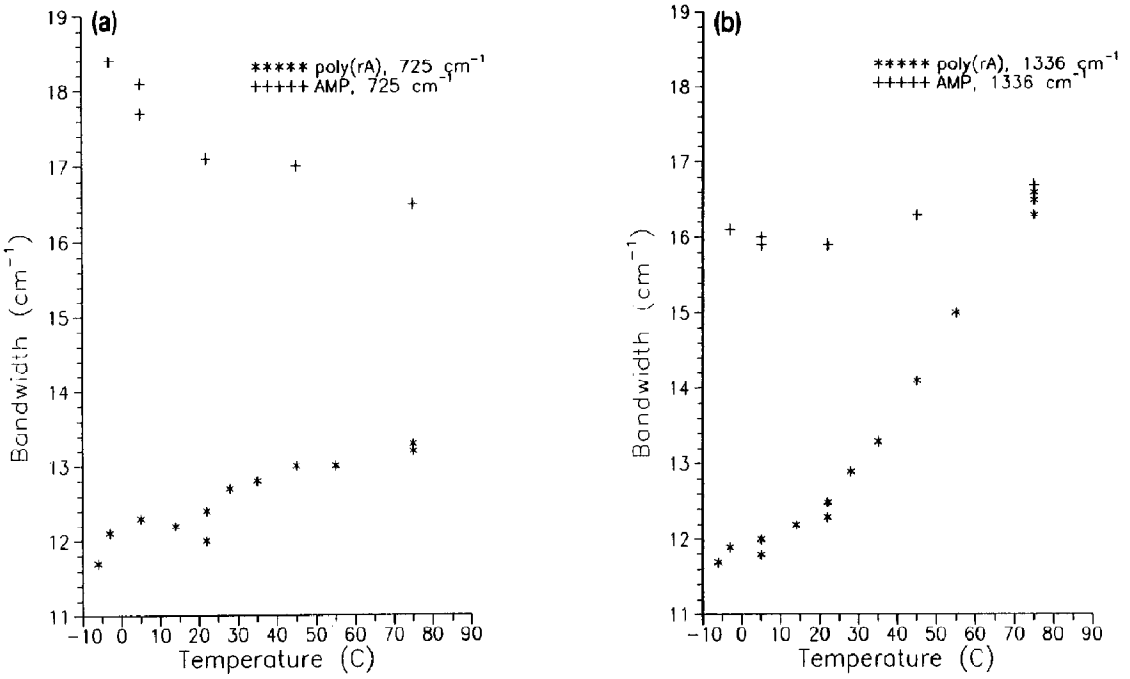

Fig. 4. (a) Temperature dependence of the bandwidths of the adenine base vibration at 725 cm^{-1} of poly(rA) and rAMP. The bandwidth of this vibration is weakly dependent on the secondary structure. It is, however, sensitive to polymerization, which is shown by the large difference between the mononucleotide rAMP and the polynucleotide poly(rA). (b) Temperature dependence of the bandwidths of the adenine base vibration at 1336 cm^{-1} of poly(rA) and rAMP. The bandwidth of this vibration is very sensitive to the secondary structure. As the base vibration is more exposed to the solvent it approaches the value for the mononucleotide.

Small et al. [6,7] the hypochromic data obtained in Raman and absorption spectroscopy follow similar curves. It was suggested and qualitatively explained by them that the origin of the hypochromic effect could be traced to the interaction of the electronic transition moments. In Figure 4a and 4b the temperature dependent bandwidths are presented of the vibrations at 725 cm^{-1} and 1336 cm^{-1}. These bands were chosen because they differ in behaviour and they were easily to monitor because of their large intensities. It should be noticed that these temperature induced bandwidth changes depend strongly on the vibration of interest. The temperature dependent bandwidth changes of the vibrations at 1336 cm^{-1} and 1480 cm^{-1} in the isotropic Raman spectrum and of the vibration at 1578 cm^{-1} in the anisotropic Raman spectrum follow again a

Table 1

Raman bandwidths and integrated intensities of poly(rA). The intensities are scaled against the PO_2^- vibrational intensity (1100 cm^{-1})

Frequency (cm^{-1})	Bandwidth (cm^{-1})		Intensity (a.u.)	
	−6°C	75°C	−6°C	75°C
1578	12.2±0.4	15.2±0.1	0.370±0.009	0.610±0.008
1505	13.9±0.5	13.4±0.4	0.144±0.005	0.41 ±0.01
1480	12.9±0.4	15.9±0.3	0.75 ±0.02	0.73 ±0.02
1336	11.8±0.2	16.3±0.1	1.15 ±0.01	1.775±0.002
725	12.3±0.2	13.2±0.2	1.16 ±0.02	1.85 ±0.02

similar curve as in the absorption and Raman hypochromism measurements. The anisotropic bandwidths are not broadened by reorientational motions, so the anisotropic bandwidths will be identical to the isotropic bandwidths (see below). Within the error of the measurement and curve fitting procedure no bandwidth changes can be observed for the bands at 725 cm^{-1} and 1505 cm^{-1} (Table 1). A possible interpretation of these bandwidth changes will be presented below.

4. Discussion

A theoretical description of the bandwidths of the vibrational bands in a Raman spectrum follows the work of Gordon [11]. Rewriting the formulas for the Raman scattering process in terms of correlation functions as was done by Nafie et al. [12] enables the distinction between the isotropic and anisotropic scattering contribution. Formulae 3 and 4 result from this theory:

$$I_{iso}(\omega) \cong \langle|\alpha|^2\rangle \int_{-\infty}^{\infty} \langle Q(t)Q(0)\rangle \exp(i\omega t)\, dt, \tag{3}$$

$$I_{aniso}(\omega) \cong \int_{-\infty}^{\infty} \langle\beta(t)\beta(0)\rangle\langle Q(t)Q(0)\rangle \times \exp(i\omega t)\, dt, \tag{4}$$

where α and β are respectively the trace and the anisotropy of the polarizability tensor, Q is a normal mode and ω is the frequency in rad/s. From the measured bandwidths in the isotropic and anisotropic spectra the correlation time for reorientational motion can be obtained [13]. The trace of the polarizability is insensitive to rotations if there are no intermolecular coupling mechanisms. So the isotropic Raman bandshape is only broadened by vibrational relaxation (eq. 3), whereas the anisotropic Raman bandshape is also broadened by rotations. Thus by comparing these two bandwidths, the extra broadening in the anisotropic Raman spectrum provides information about rotations. This method works well for small molecules that have a sufficiently fast reorientational motion and a suitable structure of the scattering tensor components. This was explained in [14]. Their method was used to establish the correlation time for reorientational motion of rAMP to be 5 ps ± 1 ps. The motion of the base molecules attached to the backbone of the single stranded poly(rA) is too slow to be observable due to the large bandwidth of the vibrations and the limit of bandwidth changes which we can observe with our data analysis (±0.5 cm^{-1}). The reorientational motion of poly(rA) is apparently slower than ~10 ps (a rotation with a correlation time of 10 ps broadens an anisotropic band with 0.5 cm^{-1}).

Various processes contribute to the vibrational correlation function of a vibration in a molecule [15,16]. A general way to treat the influence of the different processes on the bandwidth is by expressing the vibrational amplitude correlation function, $\langle Q(t)Q(0)\rangle$, in terms of the correlation function of the perturbation. The work of Rothschild is followed here [15]:

$$\hat{\phi}(t) = \langle Q(t)Q(0)\rangle = \exp\left\{-\langle|\omega_1(0)|^2\rangle \int_0^t d\tau (t-\tau)\hat{\psi}(\tau)\right\}, \tag{5}$$

where $\psi(t) = \langle H_1(t)H_1(0)\rangle$, $H_1(t) = \hbar\omega_1(t)$ is the Hamiltonian describing the perturbation, and $\hat{\phi}(t)$, $\hat{\psi}(\tau)$ are normalized correlation functions. The emphasis is now shifted to the time-behavior of the frequency-shift $\omega_1(t)$. We further define the two correlation times for respectively the perturbation, τ_c, and the vibration, τ_a:

$$\tau_c = \int_0^{\infty} dt\psi(t), \tag{6}$$

$$\tau_a = \int_0^{\infty} dt\phi(t). \tag{7}$$

For a very fast perturbation ($\tau_c \ll \tau_a$) one can put $\psi(t) \cong \delta(t)$. This results in a Lorentzian band profile with a FWHM, $\Delta\nu = 2\tau_c\langle|\omega_1(0)|^2\rangle$. A very slow modulation ($\tau_c \gg \tau_a$) where $\psi(t) \cong 1$, yields a Gaussian band profile with a FWHM, $\Delta\nu = 2\sqrt{(2 \ln 2\, \langle|\omega_1(0)|^2\rangle}$.

4.1. Determination of the modulation regime

The results of our curve fit indicate that the band profiles of the adenine base vibrations are at least 90% Lorentzian, which gives a first indication that the vibrations of poly(rA) in water solution are rapidly modulated.

The second moment M(2) of a band profile $F(\omega)$ is proportional to the time independent term $\langle |\omega_1(0)|^2 \rangle$ of eq. (5) [17].

$$M(2) = \int F(\omega)\omega^2 \, d\omega / \int F(\omega) \, d\omega \qquad (8)$$

The complicated spectra of nucleotides make it difficult to get an estimate of M(2). For the calculation of M(2), the wings of a bandprofile are very important. But due to overlapping bands in Raman spectra of polynucleotides, this information is not readily available. The band at 725 cm^{-1} is, however, rather isolated, which made it possible to eliminate neighbouring bands by using the calculated curve resolved spectrum. The window for the calculation of M(2) is determined by the points where the vibrational band intensity disappears in the noise. Due to uncertainty in the borders of a band profile, M(2) is usually underestimated. As shown in Fig. 5, a lower estimate of M(2) is easily obtained, we defined the window such that there was still a definite contribution to the intensity by the vibration at 725 cm^{-1}. For the 725 cm^{-1} band of poly(rA) we calculated $M(2) \geq 250$ cm^{-2}, so $\tau_c \leq 0.13$ ps. Using the same calculation window, we did not observe any temperature dependence of the second moment of this band (< 5%). From a Lorentz FWHM one can obtain the correlation time of the vibration through $\tau_a = 1/\pi c \Delta\nu$. For the 725 cm^{-1} vibration the FWHM of 12.3 cm^{-1} gives a τ_a of 0.86 ps. Thus we determined that poly(rA) is indeed in the fast modulation regime. If poly(rA) were in the slow modulation regime, then the measured M(2) would give a FWHM ≥ 37 cm^{-1} and the band would have a Gaussian band shape.

So adenine is in the fast modulation regime, which means that the bandwidths of the vibrational modes are determined by $\Delta\nu = 2\tau_c \langle |\omega_1(0)|^2 \rangle$. Previous measurements on vibrational dynamics in water solutions yielded correlation times τ_c of 0.2–0.4 ps for the D–O vibration of HDO diluted in H_2O [16] and ~ 1 ps for pyridine vibrations in H_2O solution [18].

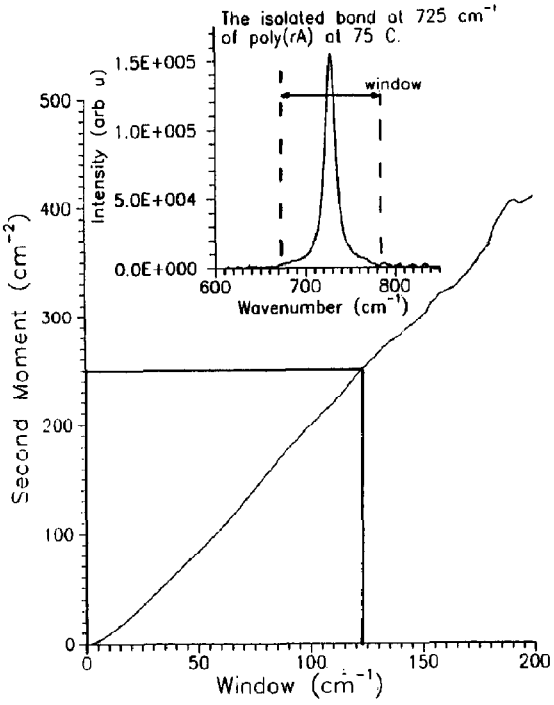

Fig. 5. The second moment for the vibration at 725 cm^{-1} of poly(rA) at 75°C as a function of the calculated window. A minimum value for the second moment of 250 cm^{-2} is obtained.

The detailed dynamical behaviour of the perturbation is determined by $\psi(t)$. Information about this function is contained in the vibrational correlation function $\phi(t)$. Due to overlapping bands we are not able to extract this kind of information from our spectra. The information contained in the bandwidth alone, however, provides a tool to elucidate different kinds of broadening processes, which will be explained below.

4.2. The temperature dependence of the bandwidths

In low density liquids and gasses, the range of interaction is a few atomic radii. Long range interactions, like dipole–dipole coupling, will be predominant in determining lineshapes. In high density liquids, however, the majority of collisions have a large impact on line broadening due to electronic overlap that causes the polarizability

distortion. A collision is here a short range interaction so that two molecules have significant electronic overlap [19]. At first we will interpret our data in terms of collisional dynamics, which causes vibrational dephasing.

The bandwidths of the adenine vibrations at 1336, 1480 and 1578 cm^{-1} increase upon melting poly(rA) (Table 1). These modes are located for a large part in the six membered ring of adenine (Table 2, [20,21]). This part of the base is furthest from the backbone, which results for the single stranded structure in a higher exposure to the solvent upon melting or a higher sensitivity to the larger mobility of neighbouring bases upon melting. We interpret this increase in bandwidth as an increase in vibrational dephasing; the $\langle |\omega_1(0)|^2 \rangle$ term for dephasing increases through a higher mobility of the bases or a decrease of shielding of the vibrations from the solvent by neighbouring bases. At 75°C, when poly(rA) is melted, the bandwidths are equal to the bandwidths in the mononucleotide rAMP. This indicates that these vibrations are completely exposed to the solvent in the melted poly(rA).

Table 2

The potential energy distributions (PED) of the normal modes

Experimental frequency (cm^{-1})	PED according to Letellier [20]			PED according to Majoube [21]		
1578				N^3-C^4	str	(28)
				$N^9C^4C^5$	ben	(15)
				C^4-C^5	str	(14)
				N^9-C^4	str[c]	(12)
1505	NC^2H	ben	(28)	N^7-C^8	str	(32)
	$C^2=N^3$	str	(15)	C^8-N^9	str	(15)
	N^1-C^2	str	(13)	C^8-H	def	(13)
	C^5-C^6	str	(10)			
1480	NC^8H	ben	(28)	C^2H	def	(31)
	$N^7=C^8$	str	(25)	C^2-N^3	str	(20)
	$C^2=N^3$	str	(12)	N^9-C^4	str	(17)
1336	NC^8H	ben	(10)[a]	C^8-N^9	str	(14)
	$C^2=N^3$	str	(8)	C^5-N^7	str	(13)
	NC^2H	ben	(8)	C^2-N^3	str	(12)
	C^8-N^9	str	(7)	N^3-C^4	str	(12)
				C^2H	def	(11)
	C^4-C^5	str	(26)[b]			
	N^1-C^2	str	(10)			
	N^3-C^4	str	(9)			
725	$C^{1'}-N^1$	str	(20)[a]	$N^9C^{1'}$	def	(21)[a]
	$C^{1'}-O^{1'}$	str	(10)	N^3-C^4	str	(7)
	$C^{1'}-N^9$	str	(15)[b]	$N^9-C^{1'}$	str	(21)[b]
	$C^{1'}-O^{1'}$	str	(10)	N^3-C^4	str	(13)
	C^4-N^3	str	(4)			
	C^8-N^9	str	(3)			
	C^6-N^1	str	(3)			
	$C^2N^1C^6$	ben	(3)			
	$C^4C^5C^6$	ben	(2)			

[a,b] means that two calculated modes have frequencies close to the experimental value; str is a stretching vibration, ben is a bending and def is a deformation.

The bandwidths of these vibrations in rAMP are insensitive, within 1 cm^{-1}, to the temperature. For a dephasing process, τ_c decreases with an increase of temperature. This would result in a narrowing of the bandwidth (motional narrowing). Apparently the decrease of τ_c is compensated by an effect in the static perturbation $\langle|\omega_1(0)|^2\rangle$. This effect is, however, impossible to identify with these measurements only.

The bandwidths of the adenine vibrations at 725 and 1505 cm^{-1} increase hardly upon melting of poly(rA). The 725 cm^{-1} vibrational bandwidth in poly(rA) remains well below the bandwidth in rAMP, whereas the 1505 cm^{-1} vibrations has the same bandwidth in poly(rA) and rAMP. The 725 cm^{-1} vibrational mode is located for a large part near the backbone [20,21], where it, even in the random coil, remains shielded from the solvent. The 1505 cm^{-1} vibrational mode, however, is located at parts which are more exposed to the solvent, and as such to solvent interaction, even in stacked poly(rA).

The bandwidth for the 725 cm^{-1} vibration in rAMP decreases with an increase of the temperature (-2 cm^{-1}). This reflects the decrease of τ_c for vibrational dephasing. To illustrate this, we model τ_c with the Enskog time τ_E [15]. The Enskog time is an improvement on the ideal gas collision time and takes finite molecular dimensions and shielding effects into account and as such models a liquid more accurate. It does not incorporate correlated or inelastic collisions.

$$\tau_E^{-1} = 4\pi\rho\sigma^2\sqrt{\frac{k_B T}{\pi M}}\left(1+\tfrac{5}{12}\pi\rho\sigma^3\right)$$
$$= \tau_E^{-1}(\rho(T), T) \qquad (9)$$

Here ρ is the number density, σ is the molecular diameter and M is the molecular mass. The τ_E for water is 0.6 ps ($\rho \cong 0.033$ Å^{-3}, $\sigma \cong 1$–1.4 Å, $M \cong 3.02 \times 10^{-26}$ kg), whereas we measured $\tau_c \leqslant 0.13$ ps. Correlated collisions, cage effects, may explain this difference. From -6°C to 75°C, eq. (9) gives a decrease of 12% of the Enskog time. The linewidth, which is a linear function of the collision time (see above), decrease 2 cm^{-1}, which is 11%. Although the Enskog approximation is a very simple model, it gives an idea of the temperature dependence of the collision time τ_c. The surprising accurate predictions for the temperature dependence may be somewhat fortuitous. We are not able to use a more sophisticated model, because we do not have any information about the detailed collisional dynamics (see above).

We also changed the polarity of the solvent for rAMP to change the static $\langle|\omega_1(0)|^2\rangle$ term. We did not observe any significant change in the bandwidths of the various vibrations (Table 3). rAMP, however, does not dissolve in the solvents

Table 3

The influence of the solvent on the bandwidths of rAMP

Solvent	Bandwidth		Dielectric constant of solvent	Polarity of solvent (D) [a]
	725 cm^{-1}	1336 cm^{-1}		
Water	17.5±0.4	16.1±0.7	78.54	1.66
Methanol (70% methanol +30% water)	18.5±1.2	15.3±0.9	32.63	1.70
Ethanol (70% ethanol +30% water)	17.0±0.7	15.3±0.8	24.3	1.69
Acetone (50% acetone +50% water)	18.0±0.8	15.1±1.3	20.7	2.88
poly(rA) (stacked, 5°C)	12.2±0.5	11.8±0.5		

[a] $D = 3.33564 \times 10^{-30}$ C m.

ethanol, methanol and acetone which we used to change the polarity of the solvent. Addition of 30% to 50% of water was necessary. This indicates that water forms a cage around the rAMP molecules and thus effectively shields them from the less polar environment, which explains the insensitivity of the bandwidths to the solvent mixture.

So far we have interpreted our data in terms of collisional dynamics. This process is certainly not the sole contributor to the vibrational bandwidth, also interbase couplings and intra-base couplings will play a role. Their influence, however, cannot be extricated from these data alone.

5. Conclusions

The study of vibrational bandwidths of poly(rA) revealed a sensitivity of these bandwidths to the secondary structure. Moreover this proved to be dependent on the vibration under study. The intensity and the bandwidth of the vibrational mode at 1336 cm^{-1} increase both upon melting of the single stranded α-helix of poly(rA). Both parameters increase towards the value of the mononucleotide rAMP. The 725 cm^{-1} vibration, however, shows a different behavior. Its intensity increases towards the value for rAMP, whereas its bandwidth hardly changes upon melting and remains below the value for rAMP. The linewidth changes were explained by the degree of exposure to the solvent. A high exposure results in a large bandwidth.

The timescales of the perturbations on the vibrational mode at 725 cm^{-1} were approximated from its bandwidth and second moment. The timescales of these processes are smaller than 0.13 ps, which is fast compared to the vibrational lifetimes of the adenine base vibrations. Part of our observations can be explained with collisional dynamics, but other processes like resonant vibrational exchange may also play a role.

It is shown that changes in (sub)picosecond dynamics of polynucleotides can be monitored with spontaneous Raman spectroscopy.

Acknowledgement

This work is supported by the Netherlands Organization for the Advancement of Pure Research (N.W.O.).

References

1 A. Schenzle and R.G. Brewer, Phys. Rev. A 14 (1976) 1756.
2 P.R. Berman, Adv. Atom. Mol. Phys. 13 (1977) 57.
3 H.G. Purucker and A. Laubereau, contribution to XII European CARS Workshop, Villigen, Switzerland, March 22–23, 1993, p. V6.
4 A. Lau, M. Pfiffer and W. Werncke, Il Nuovo Cimento, 14 (1992) 1023.
5 H. Okamoto and K. Yoshihara, Chem. Phys. Lett. 77 (1991) 568.
6 E.W. Small and W.L. Peticolas, Biopolymers, 10 (1971) 1377.
7 E.W. Small and W.L. Peticolas, Biopolymers, 10 (1971) 69.
8 K.T. Gillen and J.E. Griffiths, Chem. Phys. Lett. 17 (3) (1972) 359.
9 K. Fukushi and M. Kimura, J. Raman Spectrosc., 8 (3) (1979) 125.
10 F.F.M. de Mul, H.B.G. ten Have, C. Otto and J. Greve, J. Raman Spectrosc., 21 (1990) 725.
11 R.G. Gordon, Adv. Magn. Reson., 3 (11) (1968) 1.
12 L.A. Nafie and W.L. Peticolas, J. Chem. Phys. 57 (8) (1972) 3145.
13 F.J. Bartoli and T.A. Litovitz, J. Chem. Phys. 56 (1) (1972) 404.
14 F.J. Bortoli and T.A. Litovitz, J. Chem. Phys. 56 (1) (1972) 413.
15 W.G. Rothschild, Dynamics of molecular liquids (Wiley, New York, 1984).
16 C.H. Wang, Mol. Phys. 33 (1) (1977) 207.
17 W.G. Rothschild, J. Chem. Phys., 65 (1) (1976) 455.
18 W. Schindler and H.A. Posch, Chem. Phys. 43 (1979) 9.
19 R.H. Clarke and S. Ha, Spectrochimica Acta, 43A (11) (1987) 1385.
20 R. Letellier, M. Ghomi and E. Taillandier, J. Biomol. Struct. Dyn., 4 (4) (1987) 663.
21 M. Majoube, Biopolymers 24 (1985) 2357.